

# Nitrogen-15 NMR spectroscopy of sugar sensor with B–N interaction as a key regulator of colorimetric signals

Yuya Egawa, <sup>\*1</sup> Yoshiyuki Tanaka, <sup>2</sup> Ryota Gotoh, <sup>2</sup> Satoshi Niina, <sup>2</sup> Yu Kojima, <sup>1</sup> Naoki Shimomura, <sup>1</sup> Hiroko Nakagawa, <sup>1</sup> Toshinobu Seki, <sup>2</sup> and Jun-ichi Anzai<sup>2</sup>

<sup>1</sup> Faculty of Pharmaceutical Sciences, Josai University, Keyakidai, Sakado, Saitama 350-0295

<sup>2</sup> Graduate School of Pharmaceutical Sciences, Tohoku University, Aobayama, Aoba-ku, Sendai, Miyagi 980–8578

(Received <Month> <Date>, <Year>; CL-<No>; E-mail: <yegawa@josai.ac.jp>)

Nitrogen-15 NMR spectroscopy showed strongly upfield values of the chemical shift for one of the azo nitrogen atoms of a boronic acid appended azo dye; this indicated the formation of a boron–nitrogen (B–N) dative bond. The B–N dative bond was cleaved by sugar addition.

Boronic acids are widely used for sugar sensors because they react with diol moieties of sugars to form boronate esters.<sup>1</sup> Sugar sensors based on boronic acids require the occurrence of signal changes upon sugar binding. James *et al.* have developed a novel fluorescent sensor that contains a nitrogen atom at a position adjacent to the boronic acid group.<sup>2</sup> The sensor compound shows a significant increase in fluorescent intensity upon sugar binding. They proposed that the fluorescent intensity of the sugar sensor was controlled by a boron–nitrogen (B–N) interaction. Since then, the B–N motif has been widely used not only in fluorescence sensors but also in electrochemical and colorimetric sensors.<sup>3</sup> In previous studies, our group has synthesized a colorimetric sugar sensor based on the B–N interaction between boronic acid and azo groups.<sup>4</sup>

Although B–N interactions have been recognized as the key regulators of many sensor signals, there are few ways to investigate B–N interactions in solution state, except for <sup>11</sup>B NMR spectroscopy.<sup>5</sup> Unfortunately, <sup>11</sup>B NMR is not able to provide conclusive evidence for the B–N interaction because <sup>11</sup>B chemical shifts only suggest a difference in the hybridization states of boron atoms. When a boron atom is tetrahedral, its chemical shift is upfield from that of the trigonal planar geometry, where pure sp<sup>3</sup> and sp<sup>2</sup> are approximately 0 and 30 ppm, respectively.<sup>5</sup> In many cases, adding sugar induces a change in <sup>11</sup>B NMR spectra of sugar sensors, and this change is interpreted as a change in the B–N interaction. However, it is very difficult to identify the state of the B–N interaction from the limited information about boron hybridization because not only the adjacent nitrogen but also hydroxides, solvent molecules, and sugars interact with the boronic acid group, and all of these interactions are reflected in <sup>11</sup>B chemical shifts. Consequently, B–N interactions of sugar sensors have been investigated and debated for a long time.<sup>5,6</sup>

In order to gain insight into B–N interactions of sugar sensors, we utilize <sup>15</sup>N NMR spectroscopy because the formations of coordination bonds are sensitively reflected in the <sup>15</sup>N chemical shifts.<sup>7</sup> We synthesized a <sup>15</sup>N-labelled boronic acid-appended azo dye (<sup>15</sup>N-BA, Figure 1 (a)) which shows the same character as the colorimetric sugar sensors reported previously.<sup>4</sup> We measured its <sup>15</sup>N NMR spectra and conducted density function theory (DFT) calculations to

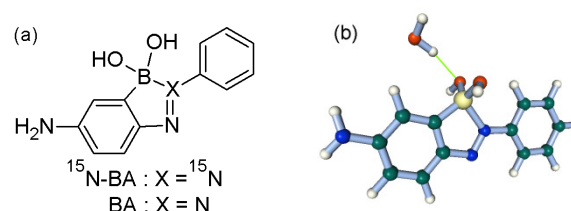


**Figure 1.** (a) Structures of <sup>15</sup>N-BA and BA, (b) An energy minimized structure of BA containing a hydrogen bond with a water molecule. Hydrogen bonds are shown in light green.

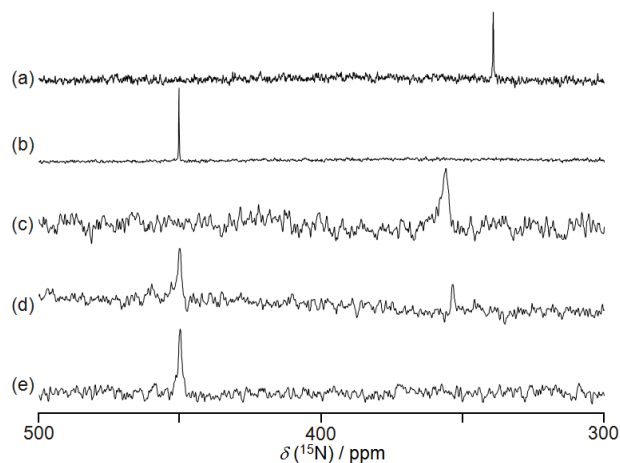
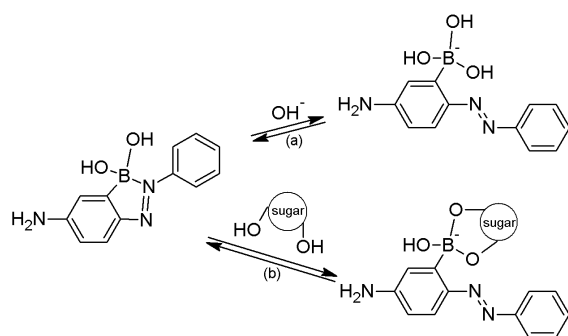


**Figure 2.** <sup>15</sup>N NMR spectra of <sup>15</sup>N-BA (20 mM) under various conditions: (a) in D<sub>2</sub>O, (b) in a 1.0 M NaOD D<sub>2</sub>O solution, (c–e) in a mixed solvent (100 mM CHES buffer pH 10.0/DMSO-*d*<sub>6</sub> = 3/1, v/v), (c) without D-fructose, (d) in the presence of 0.10 M D-fructose, and (e) in the presence of 1.0 M D-fructose. The <sup>15</sup>N-frequency (0 ppm) is 81.07646745 MHz.

confirm the validity of the <sup>15</sup>N chemical shifts values.

Figure 2 (a) shows the <sup>15</sup>N NMR spectra of <sup>15</sup>N-BA in D<sub>2</sub>O. The <sup>15</sup>N chemical shift was observed at 339 ppm; this value is strongly upfield shifted because <sup>15</sup>N chemical shifts of azo groups are generally observed at around 500 ppm.<sup>8</sup> On the other hand, the <sup>15</sup>N chemical shift of <sup>15</sup>N-BA in a 1.0 M NaOD D<sub>2</sub>O solution was observed at 450 ppm (Figure 2 (b)).

Since non-labeled boronic acid-appended azo dye (BA) acted as a colorimetric sensor at pH 10.0 (Figure 3 (b)), we investigated the effect of sugar on <sup>15</sup>N-BA in a mixed solvent (100 mM CHES buffer pH 10.0/DMSO-*d*<sub>6</sub> = 3/1, v/v). In the absence of sugar, the <sup>15</sup>N chemical shift was strongly upfield shifted (Figure 2 (c)). In the presence of 0.10 M D-fructose,



**Scheme 1.** (a) Acid-base equilibrium of BA and (b) equilibrium of BA and sugar in pH 10.0.

there were two distinct peaks at 353 and 450 ppm (Figure 2 (d)). Further addition of D-fructose extinguished the peak at 353 ppm (Figure 2 (e)).

Then, we investigated the structure responsible for the strongly upfield shift for one of the azo nitrogen atoms. We used the Gaussian suite of programs using DFT calculations at the B3LYP/6-311++G(2d,p) level of theory.<sup>9</sup> We conducted calculations of various structures and predicted their  $^{15}\text{N}$  chemical shifts. We found that the structures which did not contain a B–N dative bond showed a predicted value of around 450 ppm (Figure S1, Table S1)<sup>10</sup>. In contrast, the calculated structures that contained the B–N dative bond (Figure 1 (b) obtained with Facio software<sup>11</sup>) showed a predicted value of 349 ppm, which is in the best agreement with the actual measured value (339 ppm). Such an upfield value was reported to be found in protonated azobenzene (360 ppm), in which the azo group coordinates with a proton.<sup>8</sup> Hence, it is reasonable to conclude that the strongly upfield value of the  $^{15}\text{N}$  chemical shift is due to the existence of the B–N dative bond.

We assumed that  $^{15}\text{N}$ -BA in alkaline solutions has a boron atom coordinating with three hydroxyl groups because abundant hydroxide can coordinate with the boronic acid group. The energy-minimized structure shows a predicted value of 444 ppm (Table S1 (a))<sup>10</sup>, which agrees well with the actual measured value of  $^{15}\text{N}$ -BA in 1.0 M NaOD solution (450 ppm). On the basis of these  $^{15}\text{N}$  NMR and DFT calculation results, an acid-base equilibrium of  $^{15}\text{N}$ -BA can be presented as shown in Scheme 1(a).

On the basis of the structural information obtained from  $^{15}\text{N}$  NMR and DFT calculation results, we can explain the reason for the change in the  $^{15}\text{N}$  chemical shift of  $^{15}\text{N}$ -BA upon sugar binding in the following manner. In the condition of Figure 2 (c), the major species of  $^{15}\text{N}$ -BA has the B–N dative bond, which is responsible for the upfield value of the  $^{15}\text{N}$  chemical shift (356 ppm). Adding sugar induces a B–N dative bond cleavage, which results in a recovery of the  $^{15}\text{N}$  chemical shift in the normal range (450 ppm). This structural change (Scheme 1 (b)) corresponds to a solvolysis mechanism, which was originally proposed by Wang's group.<sup>6a,b</sup>

We also measured  $^{11}\text{B}$  NMR spectra under the same conditions as that for the  $^{15}\text{N}$  NMR spectra. In the absence of sugar, the  $^{11}\text{B}$  chemical shift was observed at 13.0 ppm (Figure S2 (c))<sup>10</sup>. Addition of D-fructose increased the  $^{11}\text{B}$  chemical shift to around 8 ppm and decreased that around 13 ppm (Figure S2 (d, e))<sup>10</sup>. Since both the  $^{11}\text{B}$  chemical shifts at around 13 and 8 ppm correspond to quasi-tetrahedral boron, it

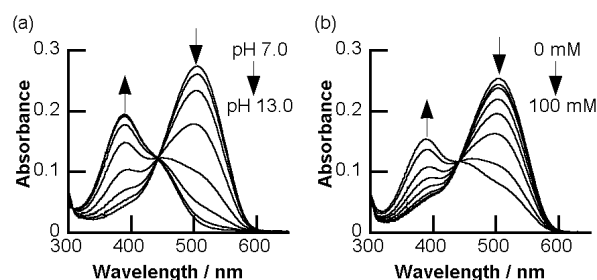


**Figure 3.** (a) UV-visible absorption spectra of BA (10  $\mu\text{M}$ ) in different pH solutions (pH 7.0, 10.0, 10.5, 11.0, 11.5, 12.0, 12.5, and 13.0), measured in a methanol/water mixture (1/1, v/v) containing HEPES (5.0 mM). (b) UV-visible absorption spectra of BA (10  $\mu\text{M}$ ) in the presence and absence of D-fructose (0, 1, 2, 5, 10, 20, 50, and 100 mM), measured in a methanol/water mixture (1/1, v/v) containing CHES (5.0 mM), pH 10.0.

is very difficult to describe the effect of sugar on the structures of  $^{15}\text{N}$ -BA.

Figure 3 shows the effect of pH and sugar on UV-visible absorption spectra of BA. In the pH range from 7 to 10, the absorption maximum was observed at 505 nm, which is significantly red-shifted compared to that of 4-aminoazobenzene (365 nm).<sup>12</sup> A pH increase induced a decrease in the absorption maximum at 505 nm and an increase in a new band at 386 nm. Sugar addition induced a similar spectral change.

From the  $^{15}\text{N}$  NMR and DFT calculation results, we can conclude that the red-shift of the absorption maximum is due to the B–N dative bond and that the B–N dative bond is cleaved by pH increase or sugar addition (Scheme 1 (a, b)). The upfield value of the  $^{15}\text{N}$  chemical shift of BA is clear evidence for the formation of the B–N dative bond. The  $^{15}\text{N}$  NMR investigation would also be applicable to other sugar sensors showing B–N interactions, in order to determine their structural details, which would contribute to further development of sugar sensors based on boronic acids.

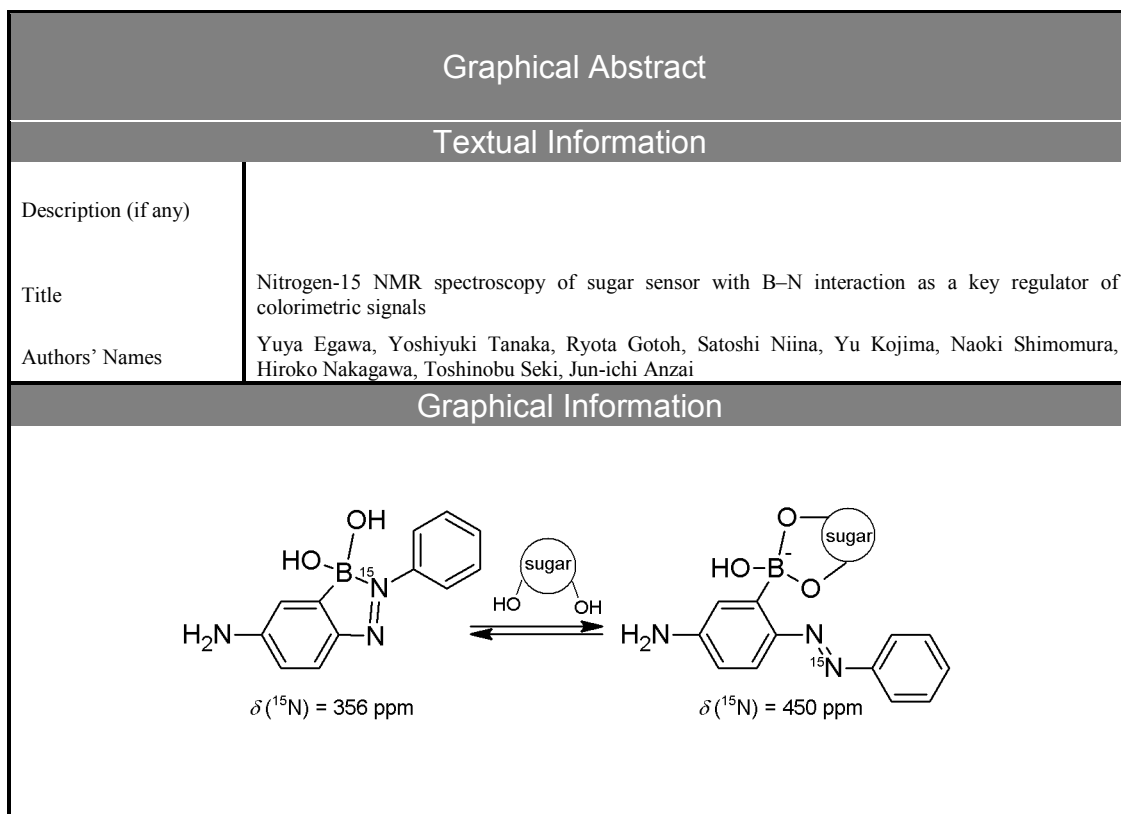
## References and Notes

- a) T. D. James, S. Shinkai, *Top. Curr. Chem.* **2002**, 218, 159. b) J. Yan, H. Fang, B. Wang, *Med. Res. Rev.* **2005**, 25, 490. c) A. Yamauchi, Y. Sakashita, K. Hirose, T. Hayashita, I. Suzuki, *Chem. Commun.* **2006**, 4312. d) C. Chimpuku, R. Ozawa, A. Sasaki, F. Sato, T. Hashimoto, A. Yamauchi, I. Suzuki, T. Hayashita, *Chem. Commun.* **2009**, 1709.
- a) T. D. James, K. R. Sandanayake, R. Iguchi, S. Shinkai, *J. Am. Chem. Soc.* **1995**, 117, 8982. b) T. D. James, K. R. Sandanayake, S. Shinkai, *Angew. Chem., Int. Ed. Engl.* **1996**, 35, 1910.
- a) S. Arimori, S. Ushiroda, L. M. Peter, A. T. Jenkins, T. D. James, *Chem. Commun.* **2002**, 2368. b) S. Arimori, M. L. Bell, C. S. Oh, K. A. Frimat, T. D. James, *J. Chem. Soc. Perkin Trans. 1.* **2002**, 803. c) C. J. Ward, P. Patel, T. D. James, *J. Chem. Soc. Perkin Trans. 1.* **2002**, 462.
- a) Y. Egawa, R. Gotoh, S. Niina, J. Anzai, *Bioorg. Med. Chem. Lett.* **2007**, 17, 3789. b) Y. Egawa, R. Gotoh, T. Seki, J. Anzai, *Mater. Sci. Eng. C.* **2009**, 29, 115.
- a) S. L. Wiskur, J. J. Lavigne, H. Ait-Haddou, V. Lynch, Y. H. Chiu, J. W. Canary, E. V. Anslyn, *Org. Lett.* **2001**, 3, 1311. b) N. Kano, J. Yoshino, T. Kawashima, *Org. Lett.* **2005**, 7, 3909. c) L. Zhu, S. H. Shabbir, M. Gray, V. M. Lynch, S. Sorey, E. V. Anslyn, *J. Am. Chem. Soc.* **2006**, 128, 1222. d) B. E. Collins, S. Sorey, A. E. Hargrove, S. H. Shabbir, V. M. Lynch, E. V. Anslyn, *J. Org. Chem.* **2009**, 74, 4055.

3

- 6 a) S. Franzen, W. Ni, B. Wang, *J. Phys. Chem. B.* **2003**, *107*,  
12942. b) W. Ni, G. Kaur, G. Springsteen, B. Wang, S. Franzen,  
*Bioorg. Chem.* **2004**, *32*, 571. c) T. D. James, *Top. Curr. Chem.*  
**2007**, *277*, 107.
- 7 Y. Tanaka, A. Ono, *Dalton Trans.* **2008**, 4965.
- 8 a) G. C. Levy, R. L. Lichter *Nitrogen-15 Nuclear Magnetic*  
*Resonance Spectroscopy*, John Wiley & Sons, Inc., New York,  
1979. b) J. Lambert, G. Binsch, J. Roberts, *Proc. Natl. Acad. Sci. U.*  
*S. A.* **1964**, *51*, 735.
- 9 Gaussian 03, Revision E.01, M. J. Frisch et al., Gaussian, Inc.,  
Pittsburgh PA, 2003. See the **Supporting Information**.
- 10 Supporting Information is also available electronically on the CSJ-  
Journal Web site, <http://www.csj.jp/journals/chem-lett/index.html>.
- 11 M. Suenaga, *J. Comput. Chem. Jpn.* **2005**, *4*, 25.
- 12 Y. Liu, Y. Zhao, Y. Chen, D. Guo, *Org. Biomol. Chem.* **2005**, *3*,  
584.

**NOTE** The diagram is acceptable in a colored form. Publication of the colored G.A. is free of charge.  
 For publication, electronic data of the colored G.A. should be submitted. Preferred data format is EPS, PS, CDX, PPT, and TIFF.  
 If the data of your G.A. is "bit-mapped image" data (not "vector data"), note that its print-resolution should be 300 dpi.



## Supporting Information

### Nitrogen-15 NMR spectroscopy of sugar sensor with B–N interaction as a key regulator of colorimetric signals

Yuya Egawa,\* Yoshiyuki Tanaka, Ryota Gotoh, Satoshi Niina, Yu Kojima, Naoki Shimomura, Hiroko Nakagawa, Toshinobu Seki, and Jun-ichi Anzai

#### Contents

#### Experimental Section

#### Theoretical Calculations

**Figure S1.** Energy-minimized structures of BA.

**Figure S2.**  $^{11}\text{B}$ -NMR spectra of  $^{15}\text{N}$ -BA

**Table S1.** Calculated values of  $^{15}\text{N}$  and  $^{11}\text{B}$  chemical shifts under various conditions.

#### References

#### Experimental Section

##### Preparation of 5-amino-2-(phenylazo)phenylboronic acid (BA):

Aniline (1.0 g, 11 mmol) was dissolved in 40 ml of 1.0 M HCl, and the solution was cooled to 0°C. Sodium nitrite (0.76 g, 11 mmol) in 10 ml of water was added to the aniline solution keeping the temperature below 5°C to prepare the diazonium salt. After 15 min, 2.0 g (11 mmol) of 3-aminophenylboronic acid in 20 ml of 1.0 M NaOH was added to the diazonium salt solution at 0°C. The mixture was neutralized by adding of a small amount of 1.0 M NaOH and stirred for 2 h at 0°C and additional 2 h at room temperature. The resulting aqueous solution was extracted with AcOEt (3×50 ml). The organic extracts were combined, washed with brine, and dried over  $\text{MgSO}_4$ . The solvent was removed in *vacuo*. The crude was purified by silica gel chromatography using  $\text{CHCl}_3/\text{MeOH}$  (10/1, v/v) as an eluent. The solvent was removed in *vacuo*. The resulting crude contained a small amount of MeOH. To remove MeOH, the following procedure was repeated three times. The crude was dissolved in water, and the water was removed in *vacuo* at 40°C to avoid thermal

decomposition of BA. As a result, BA was obtained as orange solid (0.12 g, 4.5 %); mp 156 °C (dec.); (Found: C, 59.75; H, 5.01; N, 17.43.  $C_{12}H_{12}BN_3O_2$  requires C, 59.79; H, 5.02; N, 17.43);  $\delta H$  (600 MHz;  $CD_3OD$ ;  $Me_4Si$ ) 6.66 (dd,  $J$  8.2 and 2.1 Hz, 1H), 6.75 (d,  $J$  2.1 Hz, 1H), 7.40 (t,  $J$  7.9 Hz, 1H), 7.48 (t,  $J$  7.9 Hz, 2H), 7.76 (d,  $J$  8.2 Hz, 1H), 8.06 (m, 2H);  $\delta C$  (150 MHz;  $CD_3OD$ ;  $Me_4Si$ ) 114.7, 117.6, 121.8, 130.4, 130.5, 133.2, 146.3, 149.5, 158.3. A signal due to the carbon atom directly attached to the boron atom could not be detected;  $m/z$  (FAB<sup>+</sup>) 296 ( $[M-H+glycerol-2H_2O]^+$ ).  $C_{15}H_{15}BN_3O_3$  requires 296, BA was detected as a complex with glycerol.

#### Preparation of $^{15}N$ -labeled 5-amino-2-(phenylazo)phenylboronic acid ( $^{15}N$ -BA):

$^{15}N$ -BA was synthesized in the same way using  $^{15}N$ -labeled aniline as a starting material, which was used for  $^{11}B$  and  $^{15}N$  NMR. mp 156°C (dec.),  $\delta H$  (600 MHz;  $CD_3OD$ ;  $Me_4Si$ ) 6.66 (dd,  $J$  8.5 and 2.3 Hz, 1H), 6.75 (d,  $J$  2.3 Hz, 1H), 7.40 (t,  $J$  7.4 Hz, 1H), 7.48 (t,  $J$  7.9 Hz, 2H), 7.76 (d,  $J$  8.5 Hz, 1H), 8.06 (m, 2H);  $\delta C$  (150 MHz;  $CD_3OD$ ;  $Me_4Si$ ) 114.7, 117.6, 121.8, 130.4, 130.5, 133.2, 146.3 (d,  $J^{13}C-^{15}N$  8.7 Hz), 149.4, 158.3. A signal due to the carbon atom directly attached to the boron atom could not be detected;  $m/z$  (FAB<sup>+</sup>) 297 ( $[M-H+glycerol-2H_2O]^+$ ).  $C_{15}H_{15}BN_2^{15}NO_3$  requires 297.  $^{15}N$ -BA was detected as a complex with glycerol.

#### Spectral data

##### NMR spectroscopy

The  $^1H$  NMR (600 MHz),  $^{13}C$  NMR (151 MHz),  $^{11}B$  NMR (193 MHz), and  $^{15}N$  NMR (61 MHz) spectra were measured with a JEOL ECA-600 spectrometer. Tetramethylsilane was used as an external standard for the  $^1H$  and  $^{13}C$  NMR spectra.  $Et_2O \cdot BF_3$  in toluene- $d_8$  was used as an external standard for  $^{11}B$  spectra.  $^{15}N$  chemical shift was calibrated using an indirect chemical shift referencing ratio ( $\gamma(^{15}N)/\gamma(^1H)$ ).<sup>S1,2</sup> Typical  $^{11}B$  NMR spectra were recorded at 25 °C with 16,384 complex points for 72,674 Hz (spectral width). 128 scans were averaged. Typical  $^{15}N$  NMR spectra were recorded at 25 °C with 65,536 complex points for 45,620 Hz (spectral width). 1,024 scans were averaged. The NMR samples of  $^{15}N$ -BA (20 mM) for  $^{11}B$  and  $^{15}N$  NMR measurements were prepared with various solvents. The sugar response was investigated using a mixed solvent (100 mM 2-(cyclohexylamino)ethanesulfonic acid (CHES) buffer pH 10.0/DMSO- $d_6$  = 3/1, v/v).

### **UV-Visible absorption spectroscopy**

Non-labeled BA was used in this experiment,. UV-visible absorption spectra were recorded by a Shimadzu UV-3100PC spectrometer (Kyoto, Japan). The pH titrations of BA were carried out by adding small amounts of NaOH and HCl of the solution (10  $\mu$ M BA, 5.0 mM 4-(2-hydroxyethyl)-1-piperazineethanesulfonic acid (HEPES) in H<sub>2</sub>O/MeOH). The measurement of pH using a standard electrode is not strictly applicable to 50% MeOH solutions. However, previous report shown that for solutions in 50% MeOH the pH is only changed by 0.1 of a pH unit compared to a 100% water solution.<sup>S3</sup> The sugar response of BA were studied in a pH 10 solution (10  $\mu$ M BA, 5.0 mM CHES in H<sub>2</sub>O/MeOH).

### **Theoretical calculations**

All calculations were accomplished by using the Gaussian 03 suite of programs.<sup>9</sup> The geometric optimizations of the structures and frequency analyses were carried out by using the B3LYP functional with the 6-311++G(2d,p) basis set. NMR shielding values were calculated at the B3LYP/6-311++G(2d,p) levels of theory using the GIAO method as implemented in the Gaussian 03 package. <sup>15</sup>N and <sup>11</sup>B chemical shifts were calculated using nitromethane and Et<sub>2</sub>O·BF<sub>3</sub> as references, respectively. We confirmed that no imaginary frequency was observed for all the optimized structures that were used for the calculations of the NMR shielding values.

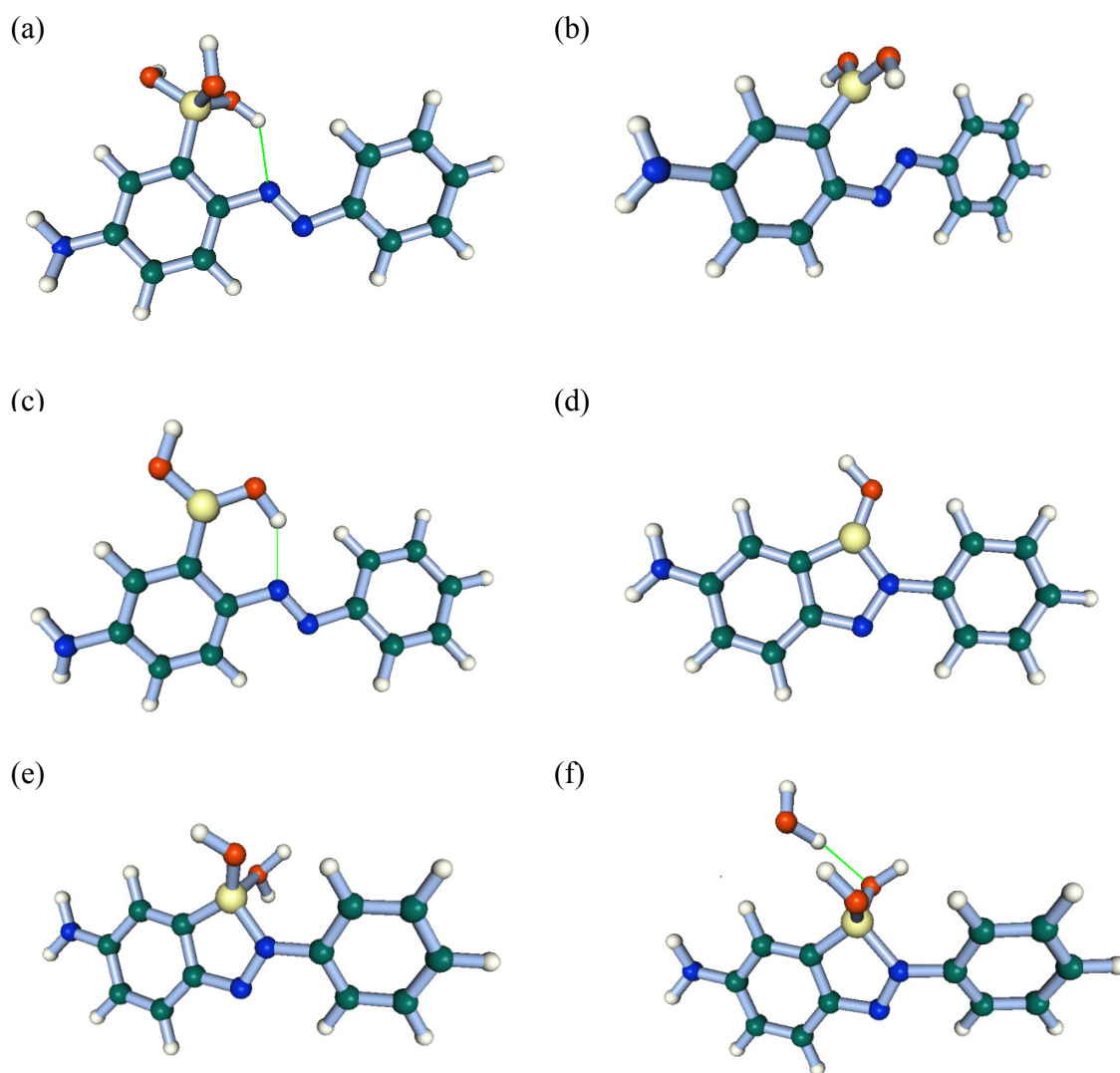


**Figure S1.** Energy-minimized structures of BA: (a) BA containing three hydroxyl groups, (b) BA without a B-N bond, (c) BA containing an intramolecular hydrogen bond, (d) dehydroxylated BA, (e) protonated BA, and (f) another structure of BA containing a hydrogen bond with a water molecule. Hydrogen bonds are shown by light green.



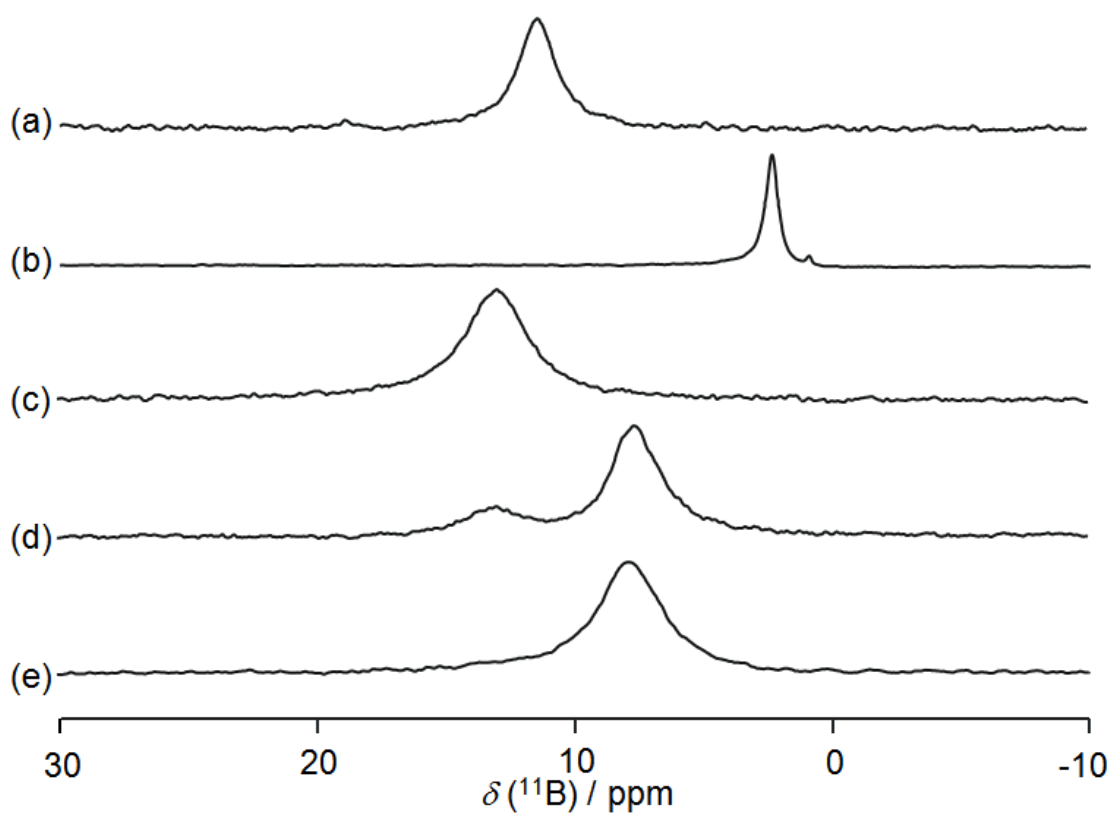


**Figure S2.**  $^{11}\text{B}$  NMR spectra of  $^{15}\text{N}$ -BA (20 mM) under various conditions: (a) in  $\text{D}_2\text{O}$ , (b) in 1.0 M NaOD  $\text{D}_2\text{O}$  solution, (c–e) in a mixed solvent (100 mM CHES buffer pH 10.0/ $\text{DMSO-}d_6 = 3/1$ , v/v), (c) without D-fructose, (d) in the presence of 0.10 M D-fructose, and (e) in the presence of 1.0 M D-fructose. The  $^{11}\text{B}$ -frequency (0 ppm) is  $\text{Et}_2\text{O}\cdot\text{BF}_3$  in toluene- $d_8$ .

**Table S1.** Calculated values of  $^{15}\text{N}$  and  $^{11}\text{B}$  chemical shifts under various conditions.\*

Entry	$^{15}\text{N}$ / ppm	$^{11}\text{B}$ / ppm
Figure 2 (b)	349	9.4
Figure S1 (a)	444	-0.6
Figure S1 (b)	465	27.5
Figure S1 (c)	468	26.5
Figure S1 (d)	242	30.3
Figure S1 (e)	262	9.8
Figure S1 (f)	312	6.2

\* $^{15}\text{N}$  chemical shifts were calculated using nitromethane and re-calibrated by using the calibration factor of 375.8 ppm (chemical shift of nitromethane with reference to liquid  $\text{NH}_3$ ).<sup>23</sup>  $^{11}\text{B}$  chemical shifts were calculated by using  $\text{Et}_2\text{O}\cdot\text{BF}_3$  as a reference.

**Geometry (Cartesian Coordinates) of BA containing a hydrogen bond with a water molecule (Figure 2 (b))**

-880.85998456 Hartree

C	-3.294125	-2.129649	-0.078654
C	-3.757345	-0.801969	0.036730
C	-2.829620	0.262456	0.132059
C	-1.479187	0.004815	0.109839
C	-1.045901	-1.328608	-0.018081
C	-1.939890	-2.398065	-0.108995
B	-0.205912	0.991109	0.184038
N	-5.104742	-0.540690	0.097573
N	0.928220	-0.389024	0.003590
N	0.329090	-1.505847	-0.064588
C	2.337500	-0.364790	-0.016919
C	2.963104	0.883569	0.063013
C	4.349958	0.956906	0.044594
C	5.115359	-0.199980	-0.052443
C	4.486554	-1.443064	-0.131475
C	3.104879	-1.533118	-0.114153
O	0.086558	1.650503	1.400362

O	0.008164	1.898478	-0.903150
H	-4.012385	-2.939008	-0.146267
H	-3.191503	1.284414	0.205138
H	-1.571844	-3.412460	-0.206771
H	-5.407463	0.408718	-0.053424
H	-5.747884	-1.249192	-0.217099
H	2.359762	1.776475	0.140083
H	4.832935	1.924449	0.107637
H	6.196867	-0.137627	-0.065914
H	5.080364	-2.346260	-0.206783
H	2.607743	-2.491108	-0.173904
H	-0.327601	1.239864	2.162573
H	-0.206451	1.517429	-1.759541
O	-2.252232	3.647491	-0.465447
H	-1.409845	3.174436	-0.601034
H	-2.048744	4.320477	0.191876

**Geometry (Cartesian Coordinates) of BA in alkaline solutions (Figure S1(a))**

-880.31197237 Hartree

C	-1.275417	-2.023980	0.007308
C	-2.606033	-2.375629	0.044913
C	-3.587835	-1.367641	0.046962
C	-3.197143	-0.030971	-0.001651
C	-1.861106	0.368394	-0.046478
C	-0.895490	-0.668506	-0.040536
N	0.446337	-0.271772	-0.086835
N	1.326935	-1.165349	0.033550
C	2.651762	-0.663601	0.027533
C	3.674343	-1.587409	-0.207961
C	5.003807	-1.182436	-0.212497
C	5.329321	0.147975	0.037564
C	4.311631	1.067801	0.294412
C	2.981464	0.673938	0.292268

N	-4.949746	-1.719140	0.043447
B	-1.501499	1.999344	-0.059849
O	-0.919272	2.282630	1.266296
O	-2.727618	2.808186	-0.245814
O	-0.615537	2.334747	-1.197323
H	-0.505103	-2.784711	0.006539
H	-2.901992	-3.420908	0.064631
H	-3.952405	0.750100	0.000061
H	3.401625	-2.620135	-0.392015
H	5.787686	-1.906488	-0.407522
H	6.366205	0.465400	0.042233
H	4.560348	2.102500	0.504643
H	2.183310	1.374187	0.504963
H	-5.554814	-0.971847	0.355914
H	-5.156622	-2.581402	0.528979
H	-1.023268	3.229097	1.409979
H	-2.695259	3.146464	-1.145177
H	0.156695	1.762733	-1.141413

**Geometry (Cartesian Coordinates) of BA without a B-N bond (Figure S1(b))**

-804.39022161 Hartree

C	3.399388	-1.764980	-0.006131
C	3.947731	-0.475314	-0.006603
C	3.077346	0.631730	-0.004048
C	1.697584	0.486697	-0.000108
C	1.173330	-0.825029	-0.000401
C	2.027149	-1.930593	-0.002481
B	0.763546	1.774037	0.006491
N	5.318789	-0.286499	-0.065071
N	-0.922252	-0.063729	-0.004927
N	-0.205982	-1.093986	0.001640
C	-2.321276	-0.259751	-0.002755
C	-3.093617	0.904629	-0.011512

C	-4.480343	0.819278	-0.010532
C	-5.100696	-0.425577	-0.000800
C	-4.328600	-1.588796	0.008012
C	-2.945334	-1.514341	0.007150
O	0.455432	2.439780	1.165489
O	0.469715	2.460623	-1.143473
H	4.054216	-2.629301	-0.012745
H	3.512992	1.627413	-0.008034
H	1.589585	-2.921626	-0.000893
H	5.665997	0.613052	0.230537
H	5.897650	-1.056338	0.233639
H	-2.587080	1.861758	-0.019105
H	-5.076014	1.724162	-0.017465
H	-6.182104	-0.494053	-0.000088
H	-4.814237	-2.557751	0.015563
H	-2.335955	-2.407740	0.013873
H	0.687355	1.944806	1.955441
H	0.718826	1.983985	-1.939531

**Geometry (Cartesian Coordinates) of BA containing an intramolecular hydrogen bond (Figure S1(c))**

-804.4006051 Hartree

C	1.399472	-1.772382	0.107092
C	2.732530	-2.115258	0.123749
C	3.724495	-1.120202	0.058581
C	3.325329	0.219354	-0.023070
C	1.984666	0.592975	-0.040583
C	1.006660	-0.427425	0.023242
N	5.064151	-1.464405	0.025182
N	-0.345403	-0.030678	0.010810
N	-1.204817	-0.945954	-0.018620
C	-2.554372	-0.528233	0.018229
C	-3.493636	-1.484473	-0.379064

C	-4.847821	-1.178602	-0.379936
C	-5.277667	0.076804	0.038906
C	-4.345320	1.024370	0.460926
C	-2.990634	0.730477	0.453202
B	1.634072	2.132703	-0.140582
O	0.362534	2.603792	-0.203501
O	2.680138	3.017768	-0.167522
H	0.636424	-2.536543	0.162761
H	3.023687	-3.158527	0.187835
H	4.081914	0.994167	-0.076179
H	5.725658	-0.739164	0.256179
H	5.314753	-2.370953	0.388495
H	-3.137531	-2.458161	-0.692177
H	-5.568456	-1.921311	-0.700581
H	-6.334608	0.314590	0.049126
H	-4.680435	1.995562	0.805586
H	-2.272627	1.459524	0.803271
H	-0.250142	1.839745	-0.165181
H	2.369902	3.927908	-0.237300

**Geometry (Cartesian Coordinates) of dehydroxylated BA (Figure S1(d))**

-728.27673064 Hartree

C	-3.643049	-1.372275	0.000457
C	-3.967358	0.004965	0.000075
C	-2.915664	0.987576	-0.000238
C	-1.618943	0.572826	-0.000169
C	-1.322413	-0.814520	0.000230
C	-2.330990	-1.788348	0.000545
B	-0.196851	1.225394	-0.000437
N	-5.247713	0.413106	0.000003
N	0.719554	0.004528	0.000054
N	0.004003	-1.091953	0.000322
C	2.138260	-0.097736	0.000033

C	2.916489	1.065055	0.000977
C	4.300780	0.958315	0.001005
C	4.911859	-0.289542	0.000101
C	4.128561	-1.444606	-0.000844
C	2.748008	-1.358621	-0.000889
O	0.261527	2.471934	-0.001007
H	-4.444504	-2.100786	0.000686
H	-3.188703	2.037943	-0.000530
H	-2.076396	-2.840788	0.000842
H	-5.490039	1.391124	-0.000325
H	-6.008289	-0.248710	0.000165
H	2.455615	2.040237	0.001729
H	4.901251	1.858985	0.001757
H	5.991732	-0.366591	0.000119
H	4.599882	-2.419260	-0.001578
H	2.141783	-2.252320	-0.001651
H	-0.394434	3.179441	-0.001325

**Geometry (Cartesian Coordinates) of protonated BA (Figure S1(e))**

-804.74927912 Hartree

C	3.651696	-1.502517	-0.091657
C	3.973755	-0.123289	-0.029872
C	2.927269	0.851013	-0.002681
C	1.625393	0.442226	-0.038892
C	1.333705	-0.943117	-0.098993
C	2.342410	-1.917600	-0.126172
B	0.201649	1.146946	-0.086995
N	5.261034	0.274961	0.007666
N	-0.711131	-0.157397	-0.133414
N	0.002583	-1.234831	-0.140000
C	-2.124059	-0.261500	-0.099591
C	-2.896934	0.868348	-0.392866
C	-4.282501	0.777926	-0.347681

C	-4.899305	-0.422996	-0.015807
C	-4.122877	-1.545505	0.271377
C	-2.740606	-1.473627	0.234075
O	-0.177956	2.187089	-0.904090
O	-0.108863	1.773845	1.503413
H	4.454523	-2.229423	-0.113432
H	3.197223	1.901026	0.051971
H	2.087645	-2.968716	-0.178453
H	5.508335	1.250462	0.039196
H	6.015799	-0.391478	-0.019454
H	-2.423000	1.788986	-0.703442
H	-4.880265	1.648170	-0.587797
H	-5.979483	-0.488128	0.016793
H	-4.600037	-2.482151	0.530944
H	-2.135089	-2.339757	0.460266
H	0.540319	2.695775	-1.291843
H	-0.216253	1.150870	2.239264
H	-0.878499	2.366858	1.489172

**Geometry (Cartesian Coordinates) of another structure of BA containing a hydrogen bond with a water molecule (Figure S1 (f))**

-880.85845782 Hartree

C	-1.997982	-2.364650	0.052888
C	-3.344782	-2.073304	0.055000
C	-3.783494	-0.729827	0.053099
C	-2.841835	0.326678	0.051042
C	-1.497640	0.049473	0.052989
C	-1.089289	-1.300876	0.052767
N	0.274220	-1.491645	0.052972
B	-0.155936	0.955723	0.078245
O	0.006713	1.674348	-1.172072
O	0.138700	1.700198	1.266903
N	-5.124462	-0.447365	0.008599



N	0.885983	-0.374459	0.100320
C	2.297185	-0.373834	0.048453
C	2.975394	0.772499	0.474070
C	4.363549	0.805288	0.425760
C	5.078937	-0.290731	-0.044227
C	4.397058	-1.430935	-0.467714
C	3.012931	-1.479246	-0.425566
H	-1.643921	-3.388552	0.054498
H	-4.078389	-2.871538	0.052589
H	-3.195884	1.353166	0.036812
H	0.839771	2.160357	-1.177001
H	-0.491727	2.422645	1.371402
H	-5.422889	0.492903	0.211870
H	-5.785273	-1.172743	0.234158
H	2.407716	1.602370	0.873648
H	4.887324	1.690445	0.766227
H	6.161100	-0.259327	-0.082802
H	4.949653	-2.285109	-0.840555
H	2.474936	-2.354949	-0.760683
O	-1.976182	3.527194	-0.404108
H	-1.320307	2.984269	-0.887085
H	-2.026648	4.364614	-0.874710

## References

Complete Reference 9:

Gaussian 03, Revision E.01,  
M. J. Frisch, G. W. Trucks, H. B. Schlegel, G. E. Scuseria, M. A. Robb, J. R.  
Cheeseman, J. A. Montgomery, Jr., T. Vreven, K. N. Kudin, J. C. Burant, J. M.  
Millam, S. S. Iyengar, J. Tomasi, V. Barone, B. Mennucci, M. Cossi, G. Scalmani, N.  
Rega, G. A. Petersson, H. Nakatsuji, M. Hada, M. Ehara, K. Toyota, R. Fukuda, J.  
Hasegawa, M. Ishida, T. Nakajima, Y. Honda, O. Kitao, H. Nakai, M. Klene, X. Li, J.  
E. Knox, H. P. Hratchian, J. B. Cross, V. Bakken, C. Adamo, J. Jaramillo, R.  
Gomperts, R. E. Stratmann, O. Yazyev, A. J. Austin, R. Cammi, C. Pomelli, J. W.

Ochterski, P. Y. Ayala, K. Morokuma, G. A. Voth, P. Salvador, J. J. Dannenberg, V. G. Zakrzewski, S. Dapprich, A. D. Daniels, M. C. Strain, O. Farkas, D. K. Malick, A. D. Rabuck, K. Raghavachari, J. B. Foresman, J. V. Ortiz, Q. Cui, A. G. Baboul, S. Clifford, J. Cioslowski, B. B. Stefanov, G. Liu, A. Liashenko, P. Piskorz, I. Komaromi, R. L. Martin, D. J. Fox, T. Keith, M. A. Al-Laham, C. Y. Peng, A. Nanayakkara, M. Challacombe, P. M. W. Gill, B. Johnson, W. Chen, M. W. Wong, C. Gonzalez, and J. A. Pople, Gaussian, Inc., Wallingford CT, 2004.

S1. Markley, J. L.; Bax, A.; Arata, Y.; Hilbers, C. W.; Kaptein, R.; Sykes, B. D.; Wright, P. E.; Wüthrich, K. *Pure & Appl. Chem.* **1998**, *70*, 117-142.

S2. For recent values, see the following

URL: [http://www.bmrb.wisc.edu/ref\\_info/cshift.html](http://www.bmrb.wisc.edu/ref_info/cshift.html)

S3. Ligny, C. De; Rehbach, S. M. *Recl. Trav. Chim. Pays-Bas*, 1960, **79**, 727.